



The Effect of Epoxidized Soybean Oil on the Physical and Mechanical Properties of PLA/PBAT/PPC Blends by the Reactive Compatibilization

Ji Eun Choo¹ · Tae Hyeong Park¹ · Seon Mi Jeon¹ · Sung Wook Hwang¹

Accepted: 3 April 2023 / Published online: 24 April 2023

© The Author(s), under exclusive licence to Springer Science+Business Media, LLC, part of Springer Nature 2023

Abstract

Poly (lactic acid) (PLA)/poly (butylene adipate-co-terephthalate) (PBAT)/poly (propylene carbonate) (PPC) multi-phase blends were prepared by melt processing technique under the presence of compatibilizer with various composition. The effect on the physical and the mechanical property with/without ESO was characterized with spectrophotometric analysis, mechanical properties, thermal properties, rheological properties and barrier properties, and the structure-properties relationship was assessed. The functional groups of PPC were found to effective to improve an interaction with carboxyl/hydroxyl group of PLA/PBAT binary blends to enhance the mechanical and physical properties on multi-phase blend system. The presence of PPC in PLA/PBAT blend affected the reduction of voids on the interface phase resulting in enhancing the oxygen barrier properties. With addition of ESO, the compatibility of ternary blend was found to be enhanced since the epoxy group of ESO reacted with the carboxyl/hydroxyl group of PLA, PBAT, and PPC, and under the condition with critical content of 4 phr of ESO, the elongation behavior dramatically increased as compared to that of blends without ESO while affecting reduction of oxygen barrier properties. The effect of ESO as a compatibilizer was clearly observed from the overall performances of ternary blends, and the potential feasibility of the PLA/PBAT/PPC ternary blends as packaging materials was confirmed at this study.

Keywords Polylactic acid · Polybutylene adipate-co-terephthalate · Polypropylene carbonate · Epoxidized Soybean Oil · Blends · Reactive compatibilization

Introduction

For the past few decades, the amount of plastic production and its waste have significantly increased, and the environmental issues have become one of the most important subjects to be resolved to achieve the sustainable eco-system and society with a great response from the plastic industries. In addition, during the COVID-19 pandemic, the waste of plastic, especially a single use disposal items used in packaging has also dramatically increased due to the fast-growing delivery market [1]. It is widely known that about 40% of plastic waste is generated from packaging materials, but increase in recycling rate of plastic waste is still in challenge. In 2019, the manufacture and consumption of plastics resulted in the emission of over 18 billion tons of greenhouse

gases, about 90% of which happened during the production and conversion process from fossil fuels.

Biodegradable polymers are good alternative to petroleum sourced plastics, and it decomposes within months to years by microorganisms under the specific composting conditions. There are various biopolymers such as bio-based/renewable resource based biodegradable polymer, poly (lactic acid) (PLA) [2–13], poly (hydroxy alkanooates) (PHAs) [14], starch and petroleum-based biodegradable polymers, polycaprolactone (PCL) [15], poly (butylene succinate) (PBS) [13, 16, 17], poly (butylene adipate-co-terephthalate) (PBAT)[9, 11, 12, 18, 19], combined polymer of both renewable and petroleum-based biodegradable polymer, poly (propylene carbonate) (PPC) [4, 6, 7, 9, 10, 19–23]. PLA, an aliphatic polyester, is the most widely used biopolymer, and monomers are usually made from fermented plant starch such as corn, wheat, casava, sugarcane and beet pulp. It is promising renewable polymer due to its mechanical and physical properties such as biocompatibility, processibility, high tensile strength, high modulus, and biodegradability

✉ Sung Wook Hwang
swhwang@kmu.ac.kr

¹ Department of Chemical Engineering, Keimyung University, Daegu, South Korea

[2, 3, 9], but the brittleness, poor toughness, slow degradation rate, and poor gas barrier property limits to a variety of packaging applications except for single-use items. PBAT is biodegradable aliphatic-aromatic co-polyester acquired from the copolymerization of adipic acid, 1,4-butanediol, and dimethyl terephthalate. Its high flexibility, thermal stability, good barrier property, and good processability [19] are welcome to be applied for the mulching film and plastic bags, however, low stiffness and weak tensile strength and modulus are still needed to be improved for the wide range of industrial applications [11, 19]. Polymer blend is common and cost-effective way to design the required properties with conventional physical procedure in plastic industry. PBAT is often blended with PLA to improve the ductility and flexibility, drawbacks of PLA. Lyu et al. reported that the improved compatibility of PLA/PBAT blends enhanced the mechanical properties, the tensile strength of 42.6 MPa, and elongation at break of more than 200% by the compatibilizer PLA-g-GMA for 3D printing applications [24] Qiu et al. had reported that the interfacial adhesion of PLA/PBAT/POSS_(epoxy)₈ (Polyhedral Oligomeric Silsesquioxane) nanocomposites could be improved with compatibilization, and the high gas barrier properties was achieved and led to extend storage period of mushrooms, strawberries and bananas [25]. Wang et al. used the epoxy-terminated branched polymer (ETBP) to enhance the compatibility of PLA/PBAT blends by developing the chemical microcrosslinked structure resulting in increase of elongation at break from 45.8 to 272% along with enhanced gas barrier property.[26] Much research has been studied to increase the compatibility of the binary blend systems by blending with other polymers and incorporating additives such as compatibilizers, chain extenders and plasticizers [24–26].

Especially, PPC is a getting attraction due to its biodegradability, transparency, and excellent oxygen barrier properties. Since poor processability and low glass transition temperature are not appropriated for industry, PPC is often blended with various biodegradable polymers such as PLA and PBAT [27]. The various compatibilizers are applied to polymer blends to improve and control the interface between polymers [28]. Pan et al. reported that the incorporation of 4,4'-methylene diphenyl diisocyanate (MDI) as chain extender on PLA/PBAT blend was very effective to enhance the mechanical properties and crystallization behavior [29]. Kim et al. investigated the effect of plasticizers such as adipate, adipic acid, glycerol ester, and adipic acid ester on PLA/PBAT blend blown film, and the interfacial adhesion was improved resulting in the better thermal and mechanical properties [11]. The influence of chain extender, Joncryl® ADR on PBAT/PPC blend was also investigated by Zhao et al., and increase in thermal stability and mechanical strength with compatibilization was achieved [23]. Song et al. reported that the effect of added TDI or TBT on PLA/

PPC mixes the copolymer effect on the improved compatibility and crystalline ability of the mixture. Adequate content of TBT and TDI improved mechanical properties over 70% PLA/30% PPC mixing by initiating transesterification of TBT and chain expansion of TDI [7]. The complementary polymer and suitable additives could enhance the properties of the polymer. Han et al. used the epoxidized soybean oil(ESO) as compatibilizer to improve compatibility and the mechanical properties such as tensile strength, elongation at break, and notched impact strength of PLA/PBAT/ESO increased sufficiently as compared to that of the PLA/PBAT composite [30].

In this study, PLA/PBAT/PPC ternary blends was manufactured by melt blending process, and the physical, mechanical and barrier properties were investigated for the potential packaging applications. In addition, the reactive compatibilization with ESO in PLA/PBAT/PPC ternary blends was performed and the compatibility of the ternary blends was evaluated by assessing the general properties. The structure-property relationship of multi-phase polymer blends was also investigated.

Experimental

Materials

PLA (LX575 grade, 98% L-isomer, with a density of $1.24\text{g}/\text{cm}^3$) was supplied by Total Energies Corbion Ltd. (Gorinchem, Netherlands) and PBAT (A400, with a density of $1.22\text{g}/\text{cm}^3$) was supplied by Zhuhai Wango Chemical Co., Ltd. (Zhuhai, China). PPC (QPAC 40 grade) was purchased from EMPOWER Materials, INC. (New Castle, DE). The compatibilizer, Epoxidized Soybean Oil (ESO), was purchased from the Sajo Daerim Ltd. (Seoul, Korea), and the chemical structures of materials used in this study are given in Scheme 1.

Sample Preparation

Prior to melt blending process, PLA, PBAT, and PPC were vacuum dried at 60°C and 30°C for 12 h, respectively, to remove residual moisture in the resin. In our previous study, 70/30 wt% composition ratio of PLA/PBAT was found to be optimized ratio to achieve the balanced properties of PLA/PBAT blends. Therefore, the PLA/PBAT composition was fixed and applied to this study. The PLA/PBAT/PPC blends with various compositions were melt mixed in an internal mixer, a Plasti-Corder® Rheometer equipped with a three-piece mixing head (Brabender, Duisburg, Germany) at 180°C with 45 rpm of rotor speed. The blend composition used in this study is presented in Tables 1 and 2. The total

Table 1 PLA/PBAT/PPC blends composition

Samples	PLA/PBAT Blends (wt%)	PPC (wt%)
LBC 0	100	0
LBC 5	95	5
LBC 10	90	10
LBC 15	85	15
LBC 20	80	20

Table 2 Compatibilizer contents on PLA/PBAT/PPC blends composition

Samples	PLA/PBAT/PPC Blends (%)	Compatibilizer (phr)
LBCS 0	100	0
LBCS 1		1
LBCS 2		2
LBCS 3		3
LBCS 4		4
LBCS 5		5

mixing time was fixed at 7 min to prevent the possible thermal degradation of the PLA, PBAT and PPC during processing. In case of PLA/PBAT/PPC ternary blend with ESO, the PLA/PBAT/PPC blends were mixed for 2 min, and then the ESO was introduced and mixed for 7 min. PLA/PBAT/PPC blend samples were taken out of the mixer and vacuum dried in an oven at 60 °C for 12 h. The compression molded sheets were prepared using a hot-press machine (CARVER, Inc. Wabash, IN, USA) at 180 °C for 3 min under 4~5 MPa pressure, and the test specimens were cooled for 3 min using water circulation aluminum blocks at 10 °C.

Characterization

Spectrophotometric Analysis

The Fourier transform infrared (FT-IR) spectroscopic analysis of PLA/PBAT/PPC blend samples was performed with a FT-IR spectrometer with ATR mode (Cary 600 Series, Agilent Technologies, Santa Clara, CA, USA). A total of 32 scans and the percent transmission mode were applied, and the tests were carried out in a 3500~350 cm⁻¹ wavenumber scan range with resolution of 4 cm⁻¹.

Thermal Properties

The thermal properties such as glass transition temperature (T_g), melting temperature (T_m), and percent crystallinity (X_c) of the blend samples with/without effective compatibilizer

were investigated with a differential scanning calorimeter (DSC 25, TA Instruments, New Castle, DE). The whole experiments were carried out under nitrogen atmosphere with a flow rate of 50 mL/min at a temperature range from -40 to 200 °C with 10 °C/min of heating rate including pre-annealing at 200 °C for 3 min, followed by cooling to -40 °C at a cooling rate of 10 °C/min. The heat of fusion (93.1 J/g) for 100% PLA was applied to determine X_c from the following equation:

$$X_c(\%) = \frac{\Delta H_m - \Delta H_c}{\Delta H_m^c(1-x)} \quad (1)$$

where ΔH_m is the enthalpy of fusion, ΔH_c is the enthalpy of cold crystallization, ΔH_m^c is the enthalpy of fusion of the pure crystalline PLA, and x is the weight fraction of PBAT and PPC. The heat of fusion (114 J/g) for 100% PBAT was also used to calculate the crystallinity of PBAT where ΔH_m^c is the enthalpy of fusion of the pure crystalline PBAT, and x is the weight fraction of PLA and PPC. The thermal stability of the blend samples was also analyzed using a thermogravimetric analyzer (TGA, Q500, TA Instruments, New Castle, DE, USA). Approximately 10 ± 2 mg of the blend samples was used, and the tests were performed at a temperature of up to 550 °C with 10 °C/min of heating rate under a nitrogen atmosphere.

Mechanical Properties

The mechanical properties such as the tensile strength, Young's modulus, and elongation at break of the blend samples were carried out with a universal testing machine (UTM, Instron 3367, Instron, Norwood, MA, USA). The specimens with dumbbell shape (ISO 37- Type 2) having a width of 3 mm and a gauge length of 2 mm were cut from specimen cutter. The mechanical property was tested at room temperature with a cross-head speed of 50 mm/min. At least 7 specimens were selected from each sample except maximum and minimum value, and the average value and standard deviation was obtained.

Melt Flow Index

The melt flow index of the neat PLA, PBAT and PPC was measured with a melt flow indexer (mi-2 series, GÖTTFERT, Buchen, Germany). All samples were performed at 180 °C, actual processing temperature with a 2.16 kg load. The samples were cut every 2 min, and the average values of three measurements were reported.

Morphological Observation

The micro-structure and morphology of fractured surface of blends were identified using the field-emission scanning

electron microscopy (FE-SEM) (SU8020, Hitachi, Tokyo, Japan). Compression molded sheets were fractured after being frozen in liquid nitrogen to prevent deformation during fracture, and then all samples were sputter-coated via an ion sputter coater (E-1045, Hitachi, Tokyo, Japan) under vacuum conditions with conductive carbon tape. Test was performed under high vacuum with the acceleration voltage of 3.0 kV.

Contact Angle Analysis

A static contact angles of PLA, PBAT, and PPC were measured using a contact angle analyzer with a digital microscope (Phoenix-Mt, Surface Electro Optics, Suwon, South Korea). A constant volume (100mL) of sessile droplet with water and CH_2I_2 were delivered to the surface of each blend sheets by a needle of a syringe with a pump. The Harmonic mean equations were used to determine the surface free energy. The H_2O ($r_1 = 72.8 \text{ mJ/m}^2$, $r_1^d = 22.1 \text{ mJ/m}^2$, $r_1^p = 50.7 \text{ mJ/m}^2$) and CH_2I_2 ($r_2 = 50.8 \text{ mJ/m}^2$, $r_2^d = 44.1 \text{ mJ/m}^2$, $r_2^p = 6.7 \text{ mJ/m}^2$) was assessed as liquid probe on PLA/PBAT/PPC blends. Seven samples examined for each specimen.

Rheological Analysis

The melt-rheological behaviors of blend samples were analyzed with a rotational rheometer (Model: Physica MCR302, Anton Paar GmbH, Austria) using parallel-plate geometry at 190 °C. The disk diameter of the blend sheets is 25 mm with 1 mm of the thickness. All the samples were vacuum dried at 60 °C for 24 h before testing, and tests were performed at 190 °C under a nitrogen atmosphere. The dynamic frequency sweep test over a frequency range of 0.1 ~ 100 rad^{-1} was applied.

Barrier Properties

The oxygen barrier properties of blend samples were analyzed by the oxygen permeation analyzer (OX-TRAN 702, MOCON, Brooklyn Park, MN) complying with ASTM 3985. The aluminum masks (5 cm^2) were used to prepare the test specimens, and the permeation test was performed under the condition of 23 °C and 0% relative humidity (RH) under atmosphere pressure.

Statistical Analysis

Statistical analyses of PLA/PBAT/PPC ternary blend with/without ESO data were determined with SPSS software (SPSS Inc., Chicago, IL, USA). Oneway analysis of variance using the general linear model procedure were used to determine significant differences ($\alpha < 0.05$)

Results and Discussion

Effect of PPC on PLA/PBAT Binary Blends

Spectrophotometric Analysis

The FT-IR spectra results of blend samples were given in Fig. 1. The stretching vibration peak of the hydroxyl group appears between 2900 and 3000 cm^{-1} since PLA, PBAT, and PPC all include OH groups as part of their molecular end groups. The adsorption peak bands at 1737 cm^{-1} correspond to the strong and sharp C = O stretching vibration of pure PPC in amorphous region. The ester groups of PLA and PBAT indicate a stretching vibration of carbonyl adsorption peaks at 1711 cm^{-1} and 1748 cm^{-1} , respectively. The distinctive benzene ring structure of PBAT relates to C=C at the absorption peak of 1226 cm^{-1} . The corresponding absorption peak of carbonyl stretching was found to be shifted to lower wavenumber indicating that there were some chemical interactions such as Van der Waals interactions among PLA, PBAT, and PPC. In addition, the absorption peak for hydroxyl group was also shifted to the higher wavenumber with addition of PPC indicating the formation of hydrogen bonding among polymer chains. Alitotta et al. reported that the peak shift of carbonyl stretching could be related to the addition of PPC arising the slight alteration of average dipole distribution around the carbonyl groups in PLA, supporting the interaction of the PBAT and PPC in PLA matrix.[31].

Thermal Properties

The DSC thermogram of the neat PLA, PBAT, PPC and their blends are presented in Fig. 2; Table 3. The T_g of each neat PLA, PBAT and PPC was found to be 55.72 °C, -35.94 °C, and 25.50 °C, respectively. The compatibility of blends could be identified from the T_g shift behavior with comparison to their original values. The T_g values representing PLA of the blend samples were found to be shifted to lower temperature from 57.74 °C to 52.66 °C as PPC contents gradually increase from 0 to 20 wt%. This could indicate the partial compatibility among PLA and PPC. It also could be attributed to the increase of free volume in the blends with addition of amorphous PPC resulting in more active chain mobility in the blends. Pan et al. reported that the PBAT were well compatible with PLA chains in the amorphous region in the PLA/PBAT blend [29]. The X_c of blends was found to be significantly reduced by the addition of PPC indicating that the crystal growth and lamella arrangement of the PLA molecular

Table 3 T_g , T_{cc} , T_m , X_c of neat PLA, neat PBAT, neat PPC, PLA/PBAT/PPC Blends

Samples	T_g (PLA)(°C)	T_g (PBAT)(°C)	T_g (PPC)(°C)	T_{cc} (°C)	T_m (PLA)(°C)	T_m (PBAT)(°C)	X_c (PLA)(%)	X_c (PBAT)(%)
neat PLA	55.72 ± 0.27 ^{bc}	–	–	103.74 ± 0.24 ^a	168.1 ± 0.06 ^a	–	4.35 ± 0.49 ^a	–
neat PBAT	–	–35.94 ± 0.17	–	–	–	119.43 ± 0.07	–	12.47 ± 0.39
neat PPC	–	–	25.50 ± 0.44	–	–	–	–	–
LBC 0	57.74 ± 0.73 ^a	–	–	99.77 ± 2.58 ^{abc}	166.99 ± 0.26 ^{bc}	–	30.16 ± 1.75 ^c	–
LBC 5	56.82 ± 0.15 ^{ab}	–	–	101.40 ± 0.16 ^{ab}	167.44 ± 0.16 ^b	–	9.83 ± 0.38 ^b	–
LBC 10	55.65 ± 0.01 ^{bc}	–	–	100.80 ± 0.06 ^{ab}	167.06 ± 0.07 ^b	–	9.70 ± 0.29 ^b	–
LBC 15	54.56 ± 0.35 ^c	–	–	97.94 ± 0.20 ^{bc}	166.44 ± 0.16 ^{cd}	–	9.41 ± 0.33 ^b	–
LBC 20	52.66 ± 0.78 ^d	–	–	96.37 ± 0.42 ^c	165.98 ± 0.13 ^d	–	11.09 ± 0.49 ^b	–

Values in the same column with different superscript letters are different at $\alpha = 0.05$

chain was hindered by the amorphous chain of PPC as compared to that of PLA/PBAT blends. In one study, X_c was increased in PLLA/PPC blend, indicating that high chain motion and intermolecular rearrangement were induced [10]. On the contrary, when the amorphous PPC added to the semi-crystalline PLA/PBAT blends, chain arrangement could be partially interrupted and then the X_c of blends could be reduced.

The TGA thermograms of PLA, PBAT, PPC and blend samples were shown in Fig. 3. It was found that the addition of PPC on the blends had a profound effect on decreasing the onset decomposition temperature due to relatively poor thermal stability of neat PPC. It is reported that chain unzipping and random chain scission were two major decomposition mechanisms for PPC [19]. Cui et al. also investigated the thermal degradation behaviors of PPC with PPC/PVA blend, and found that the thermal stability of the PPC/PVA were significantly reduced under the presence of water and the hydroxyl groups in the blend [22]. As the PPC content increased, the onset decomposition temperature gradually further reduced in the blends, but overall thermal stability was found to be remained around 380–400 °C ranges, which is similar to that of PLA having much better stability as compared to that of PPC. This could be seen that the thermal stability of the blends with up to 20 wt% of PPC followed the decomposition behavior of PLA suggesting that the potential feasibility of the PLA/PBAT/PPC blend as a packaging material in a variety of applications.

Table 4 Tensile strength, Elongation at break for PLA/PBAT/PPC Blends

Samples	Young's modulus (Gpa)	Tensile Strength (Mpa)	Elongation at break (%)
LBC 0	1.25 ± 0.08 ^a	36.54 ± 1.18 ^a	19.88 ± 2.50 ^a
LBC 5	1.26 ± 0.08 ^a	39.5 ± 1.16 ^b	14.44 ± 1.12 ^b
LBC 10	1.24 ± 0.08 ^a	35.21 ± 1.70 ^a	11.38 ± 0.74 ^{bc}
LBC 15	1.31 ± 0.06 ^a	34.24 ± 0.55 ^a	11.10 ± 1.22 ^{bc}
LBC 20	1.24 ± 0.07 ^a	35.03 ± 0.51 ^a	9.80 ± 0.98 ^c

Values in the same column with different superscript letters are different at $\alpha = 0.05$

Mechanical Properties

The mechanical properties of the blends were presented in Table 4; Fig. 4. It was found that the tensile strength slightly increased from 36.54 to 39.5 MPa with addition of 5 wt% of PPC and there was no statistically significant difference up to 20 wt% of PPC maintaining the values of around 35 MPa at similar to PLA/PBAT blend. It could be concluded that the addition of PPC on the PLA/PBAT blends did not have a profound effect on the tensile strength and Young's modulus, but the elongation at break was significantly reduced from 19.88 to 9.8%. In immiscible blends, the mechanical properties were normally found to be dropped due to the poor compatibility in the interface between two polymers. In this research, poor interaction among polymers in ternary blend could lead a significant drop of elongation at break. It was reported that the viscosity mismatch of dispersed droplet phase and matrix in polymer blends could influence the morphological development during melt processing. In case that the dispersed phase having greater viscosity than matrix, full extension of molecule chain having the functional group were restricted and this could limit the interactions between phases [19].

Morphological Observation

Figure 5 presented the morphology of the neat PLA, PBAT, PPC, and blends examined from cryo-fractured surfaces of samples. The melt viscosity of polymers could

be indirectly determined from the melt flow index (MFI). The MFI values for neat PLA, PBAT, and PPC were found to be 6.97 ± 0.956 , 5.09 ± 0.01 , and 3.98 ± 0.1897 g/10min, respectively at 180 °C and 5 min preheating conditions. Since the melt viscosity of PLA was found to be lower than that of PBAT and PPC, it could be expected that PBAT and PPC could form the domains in PLA matrix with poor compatibility in interfaces. In addition, the PPC could be not only presented in domain with smaller droplet size due to lower melt flow index as compared to that of PBAT, but PPC could be interfaces between PLA and PBAT as well. The PLA/PBAT blends without PPC displayed a two-phase morphology with PBAT domain in the PLA matrix in Fig. 5D. The cavity and voids in interface between PLA and PBAT were observed indicating the poor interfacial adhesion. Chinsikikul et al. also observed similar morphology in PLA/PBAT blends with PBAT droplets with poor interfacial adhesion between the two phases [32]. Interestingly, the cohesive failures were mainly observed in simple PLA/PBAT blend showing that there were still some interactions between PLA and PBAT holding the mechanical properties, however, as the PPC content increased from 0 to 20 wt%, the adhesive failures were found with a smooth fracture surface in the PBAT domains as compared to PLA/PBAT blends with much worse interfacial adhesion. The incorporation of PPC could affect the reduction of voids, but domain-shaped cavity occurred due to weak interfacial adhesion between the domain and matrix when the sample sheets were fractured. Lins et al. illustrated that localization of a small component in blend could be theoretically approached in the ternary blend through the Young's equation that is applicable to PPC in this study. According to the following Eq. (2), r_p is the interfacial energy between PLA and PBAT. the wetting coefficient(ω_a) could be calculated and obtained [33] (Table 5).

$$\omega_a = \frac{r_{PPC/PLA} - r_{PPC/PBAT}}{r_p} \quad (2)$$

If $\omega_a > 1$, PPC is located within the PLA phase;

Table 5 Total, Polar, and dispersive components of surface energy of PLA, PBAT and PPC

Samples	Contact angle		Surface tension		
	H ₂ O (°)	CH ₂ I ₂ (°)	r _s	r ^d	r ^p
PLA	64.16 ± 0.32	40.15 ± 5.96	47.530	28.963	18.567
PBAT	66.03 ± 1.39	46.22 ± 4.50	47.007	26.547	18.460
PPC	43.19 ± 0.95	49.19 ± 3.10	56.826	23.730	33.096

Values in the same column with different superscript letters are different at $\alpha=0.05$

If $-1 < \omega_a < 1$, PPC is located at the interface of the two polymers;

If $\omega_a < -1$, PPC is located within the PBAT phase;

The calculated wetting coefficient values were found to be -0.052 , therefore it could be assumed that the PPC phase could be presented between interface of PLA and PBAT. It was confirmed that the concentration of PPC had a critical role for morphology control in ternary blends.

Rheological Analysis

Figure 6 shows the rheological properties such as the storage modulus and dynamic complex viscosity of neat PLA, PBAT, PPC and ternary blends. The neat PLA, PBAT, and PPC showed the typical Newtonian behavior in the 1 ~ 10 rad/s frequency range and exhibited non-Newtonian behavior in the low and high frequency region (0.1 ~ 1 rad/s, 10 ~ 100 rad/s). The slope in 1 ~ 10 rad/s frequency range for neat PLA, PBAT, and PPC was found to be similar, but lower slope values were observed in 0.1 ~ 1 rad/s frequency range (terminal region) for all neat polymers showing the solid-like behavior resulting from the chain entanglements. PLA/PBAT blend with PPC presenting a higher elasticity and chain entanglements, which lead to much more solid-like behavior of the blends. It could be concluded that the PPC with more flexible chain mobility resulted in increase of chain entanglement having an effect on improving the elasticity of the PLA/PBAT/PPC ternary blend. The shear thinning behavior was observed in the complex viscosity data, and PLA/PBAT samples with PPC were substantially higher viscosity than that of neat PLA, PBAT, and PPC. This increase could be related to the formation of chain entanglements between PLA, PBAT, and PPC.

Barrier Properties

Figure 7 shows the oxygen permeability of neat PPC and PLA/PBAT/PPC blends. PPC is widely known to have an excellent oxygen barrier property. It was found that the addition of PPC on the PLA/PBAT blends had an effect on reduction of oxygen permeability of the blends, and as PPC contents increased, the oxygen permeability decreased. The gas barrier property is influenced by various factors such as chemical structure of polymer, chain entanglement, and morphology developed from processing condition. As confirmed in morphological observation, PPC presented in interface between PLA and PBAT reduced the voids in interfaces. Therefore, the pathway of oxygen molecule could be decreased resulting in better oxygen barrier properties. Although the elongation and flexibility of the ternary blends still should be overcome, PPC could have a positive effect

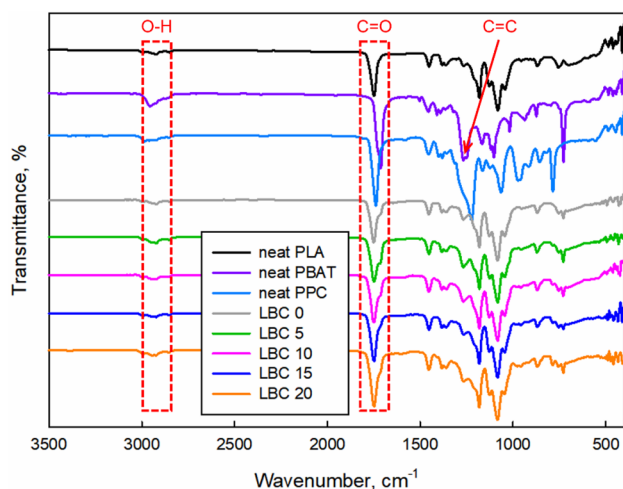


Fig. 1 Fourier transform infrared spectra of neat PLA, neat PBAT, neat PPC, PLA/PBAT/PPC Blends

on the blends, therefore the microstructure control of blends with compatibilization could be one option to achieve the balanced property as mentioned in following section.

Effect of ESO on PLA/PBAT/PPC Blends

Spectrophotometric Analysis

The FT-IR spectra of ESO and PLA/PBAT/PPC blends with ESO were shown in Fig. 8 and Scheme 2. The distinctive epoxy functional group (C-O-C) and CH₂ oscillating

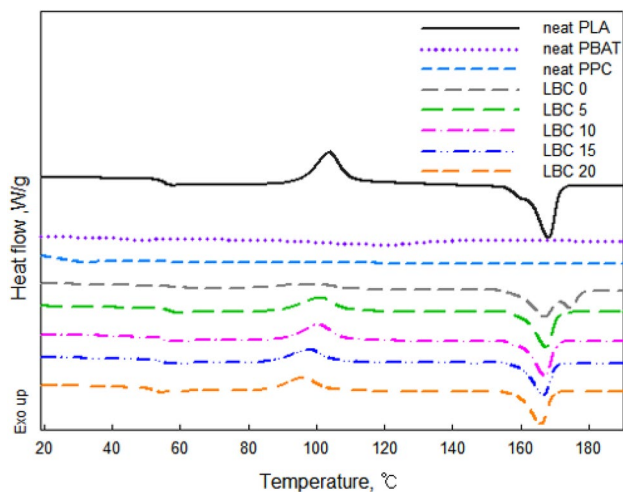


Fig. 2 TGA thermogram of neat PLA, neat PBAT, neat PPC, PLA/PBAT/PPC Blends

structure of ESO is proven by the two adsorption peaks at 822 cm⁻¹ and 724 cm⁻¹, respectively. When the ESO added, the peak increases the intensity of the carbonyl peak considerably. The epoxy groups of ESO could react with the terminal carboxyl and hydroxyl groups of PLA, PBAT and PPC forming a branched or cross-linked structure [34]. Han et al. found the similar results that ESO and PLA/PBAT blend were chemically bound to create a partly soluble branching polymer, and it was noted that the lack of absorption peaks for the distinctive epoxy group in PLA/PBAT/ESO blend. In addition, the generation of the branched structure with ESO was confirmed to be caused by the epoxy ring-opening reaction taking place between the epoxy group of ESO and the end groups of PLA/PBAT [30]. It was found that the adsorption peak of carbonyl group showed slight shift to the lower wavenumber as compared to PLA/PBAT/PPC blend without ESO. Xia et al. reported the similar phenomenon that peak shift exhibited an evident chemical reaction between the end groups of PLA/PPC and functional groups of epoxy chain extender. Jiang et al. also reported that the peak location has a slight deviation towards low wavenumber because of the interaction between hydrogen bonds [34]. The Scheme 2 presented the predicted reaction mechanism between compatibilizer and polymers.

Thermal Properties

From the DSC thermogram in Fig. 9, it was found that T_g of ternary blends representing PLA gradually decreased from 57.71 °C to 50.52 °C as the ESO content increased, and the liquid ESO could act as not only the compatibilizer but the

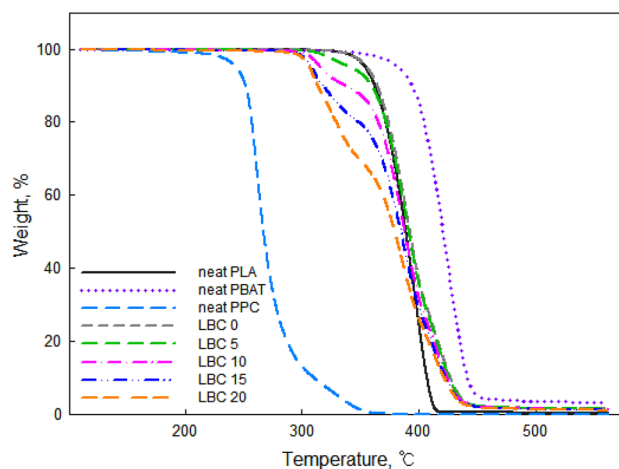


Fig. 3 DSC thermogram of neat PLA, neat PBAT, neat PPC, PLA/PBAT/PPC Blends

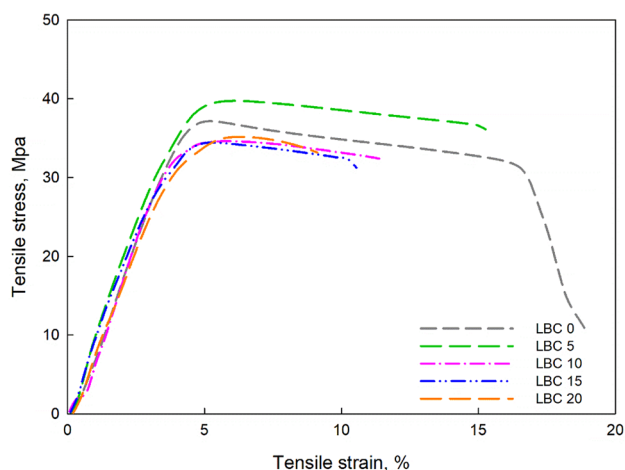


Fig. 4 Stress strain curve of PLA/PBAT/PPC Blends

plasticizer increasing chain mobility in the ternary blends as well. These results are typical for plasticized multi-phase systems and such behavior caused segmental flexibility of the polymer chains by plasticizing effect [11, 13]. The X_c of PLA/PBAT/PPC blends with ESO increased, and this could be due to molecular chain rearrangement of polymers under the state of high chain mobility from ESO addition resulting in increased chain flexibility in the blends.

The TGA thermograms of PLA/PBAT/PPC blends with ESO were shown in Fig. 10. The slight decrease of onset decomposition temperature of the ternary blend with ESO was observed, and this could be due to relatively lower thermal stability of liquid ESO. However, the initial decomposition temperature of the blends was still significantly greater than the processing temperature indicating the thermal stability would not be greatly affected by the reactive compatibilization process (Table 6).

Mechanical Properties

The mechanical properties of the blends with/without ESO were presented in Table 7; Fig. 11. There was no statistically significant difference in tensile strength up to 2 phr of ESO, and then it showed decrease tendency from 34.10 to 24.69 MPa. The addition effect of ESO in the blends on the elongation at break was found to be statistically significant. As ESO contents increased, the elongation at break enhanced dramatically from 12.75 to 49.65% up to 4 phr of ESO. This could be due to increase of the chain mobility of the PLA/PBAT/PPC by ESO. The formation of hydrogen bonding corresponding to shift of absorption peak of hydroxyl group to the higher wavenumber as confirmed in Fig. 8 could also contribute to enhanced elongation at break of the blends. Wang et al. reported that the strong physical hydrogen bonding and chemical micro-crosslinking

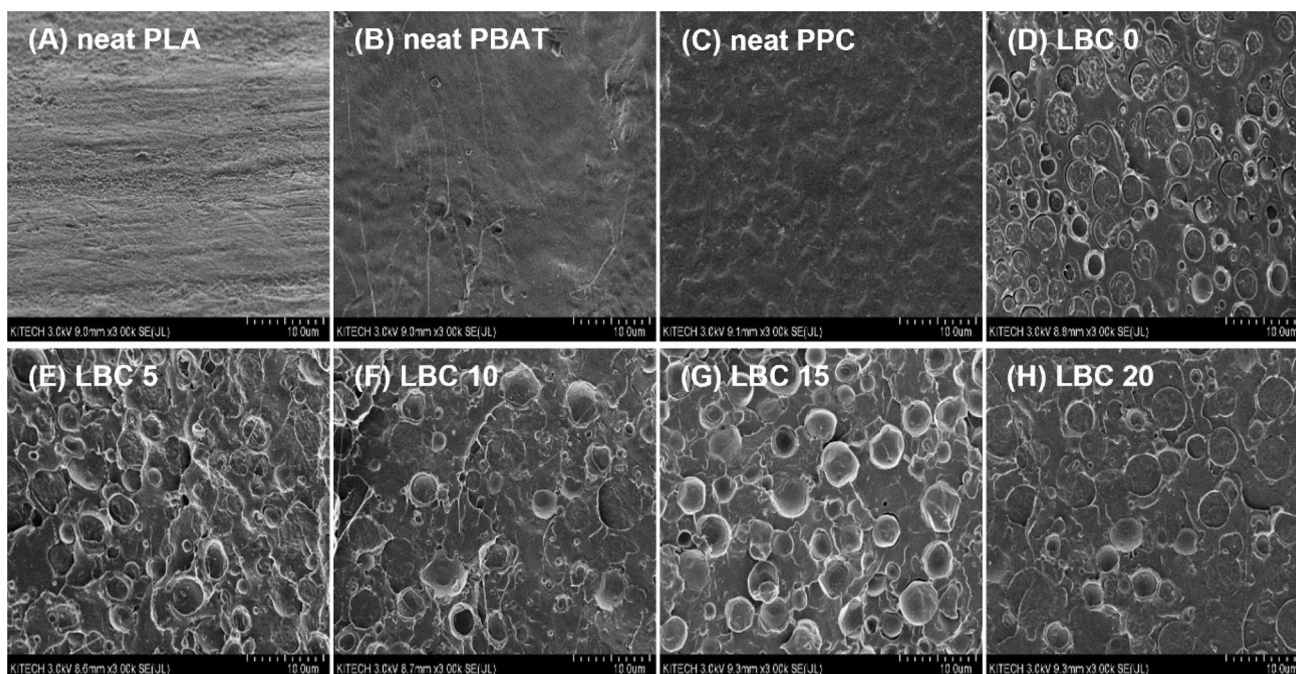


Fig. 5 SEM images cryo-fractured surfaces of neat PLA, PBAT and PPC, PLA/PBAT/PPC Blends

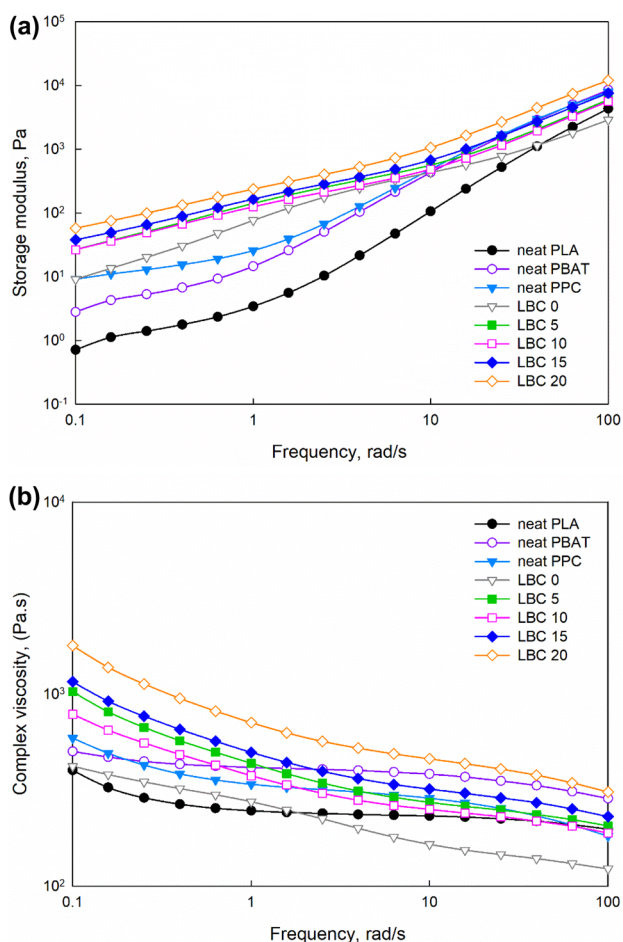


Fig. 6 Rheological properties of neat PLA, PBAT and PPC, PLA/PBAT/PPC Blends **a** storage modulus G' **b** complex viscosity η^*

interaction between the epoxy functional groups of ETBP and functional groups inside PLA and PBAT enhances the elongation at break. [26] Carbonell-Verdu et al. also observed the similar results with a PLA/PBAT blends with great improvement of elongation at break from 59.0 to 83.7% with the incorporation of 1 wt% Joncryl [35]. When ESO is incorporated into the PLA, the PLA containing 15% by weight of ESO content compared to the neat PLA had an elongation that increased from 5.1–19.2% [5]. In addition,

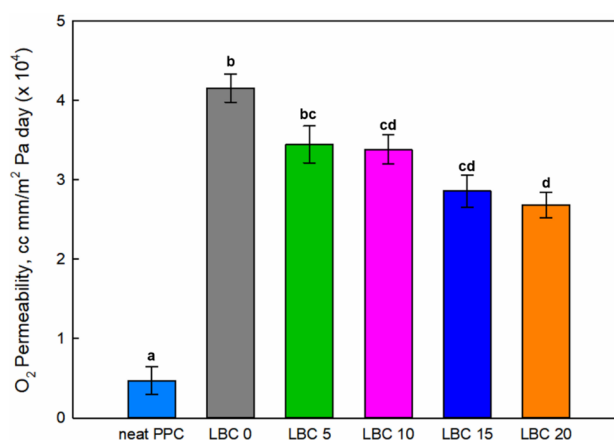


Fig. 7 Barrier properties for neat PPC, PLA/PBAT/PPC Blends

it was assumed that the partial compatibility between PPC and ESO leads to an enhance in the mechanical properties of the blend due to the chemical reaction between the epoxy group of ESO and the terminal hydroxyl group of PPC [21].

Morphological Observation

Figure 12 shows the SEM micrographs of cryo-fractured surfaces of the PLA/PLA/PPC blends with/without ESO. It was observed that the PPC presented in interfaces between PLA/ PBAT in Fig. 5 and an appropriate content of PPC could decrease the voids or cavities in the interfacial areas. As confirmed in Table 7, there is no statistically significant difference in the Young’s modulus and the tensile strength up to 2 phr of ESO contents, and a significant difference was found in the elongation at break over 3 phr of ESO contents. It was assumed that the PPC phase could be presented between interface of PLA and PBAT. PPC could be not only presented in domain with smaller droplet size due to lower melt flow index as compared to that of PBAT, but PPC could be interfaces between PLA and PBAT as well. In addition, as seen in Fig. 12, the similar phase morphology of LBCS 0 to 3 samples. However, in LCBS 3 samples, rougher surface of

Table 6 T_g , T_{cc} , T_m , X_c of PLA/PBAT/PPC blends with/without ESO

Samples	$T_{g(PLA)}$ (°C)	T_{cc} (°C)	$T_{m(PLA)}$ (°C)	$X_{c(PLA)}$ (%)
LBCS 0	57.71 ± 0.27 ^a	101.41 ± 0.10 ^a	166.80 ± 0.16 ^{ab}	9.57 ± 0.80 ^a
LBCS 1	50.96 ± 0.01 ^b	98.59 ± 0.45 ^b	166.89 ± 0.19 ^a	10.54 ± 0.38 ^a
LBCS 2	50.60 ± 0.14 ^b	96.98 ± 0.20 ^c	166.59 ± 0.15 ^{abc}	16.66 ± 0.55 ^b
LBCS 3	50.65 ± 0.15 ^b	95.80 ± 0.23 ^d	166.21 ± 0.12 ^c	16.56 ± 0.47 ^b
LBCS 4	50.74 ± 0.49 ^b	95.80 ± 0.14 ^d	166.16 ± 0.05 ^c	15.20 ± 0.26 ^c
LBCS 5	50.52 ± 0.05 ^b	95.75 ± 0.10 ^d	166.33 ± 0.11 ^b	16.80 ± 0.49 ^{bc}

Values in the same column with different superscript letters are different at $\alpha=0.05$

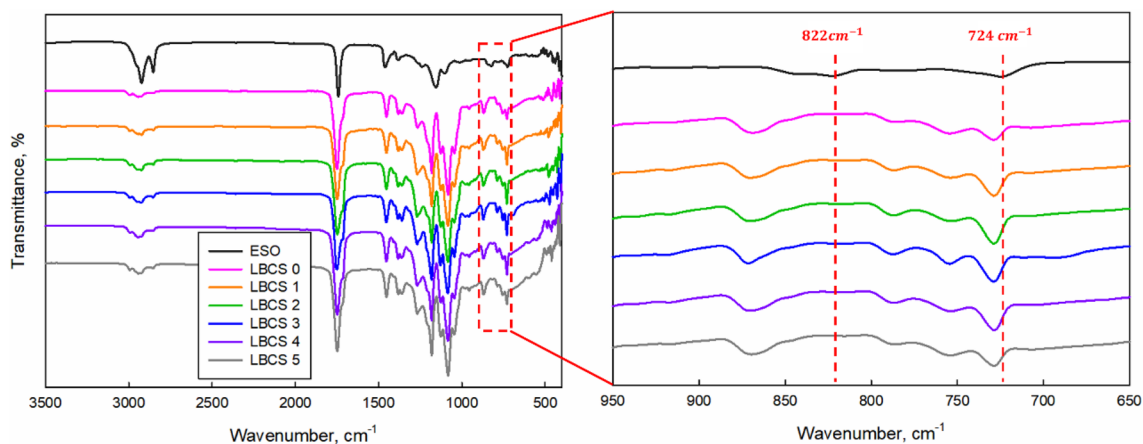
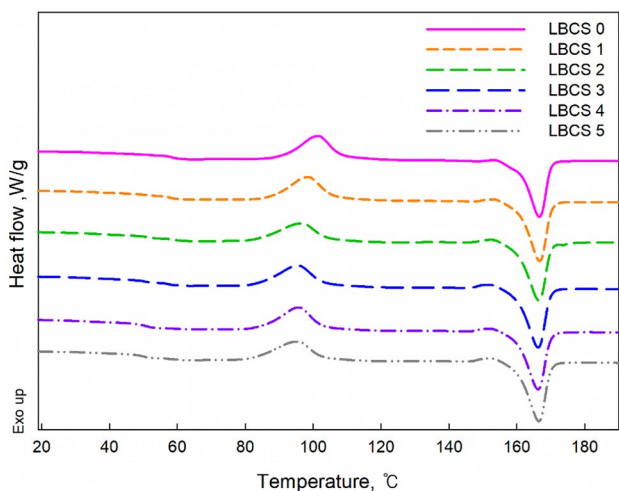
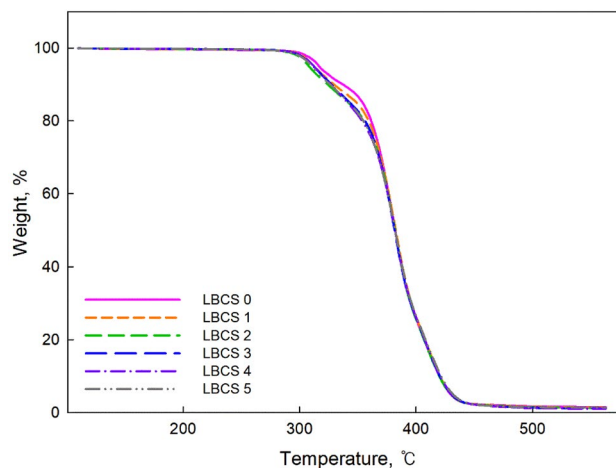
Table 7 Tensile Strength, Elongation at break for PLA/PBAT/PPC blends with/without ESO

Samples	Young's modulus (GPa)	Tensile Strength (MPa)	Elongation at break (%)
LBCS 0	0.94 ± 0.05^a	34.10 ± 0.73^a	12.75 ± 2.45^a
LBCS 1	0.95 ± 0.04^a	33.74 ± 1.15^a	17.25 ± 0.82^{ab}
LBCS 2	1.04 ± 0.08^a	34.01 ± 1.16^a	22.58 ± 1.38^b
LBCS 3	0.96 ± 0.12^a	29.30 ± 0.68^b	33.66 ± 3.65^c
LBCS 4	1.03 ± 0.08^a	28.88 ± 1.03^b	49.65 ± 4.99^d
LBCS 5	0.95 ± 0.07^a	24.69 ± 0.46^c	44.07 ± 4.33^d

Values in the same column with different superscript letters are different at $\alpha=0.05$

PBAT domain as compared to that of LBCS 1 and LBCS 2 indicating the interface interaction. In case of LCBS 4 to 5 samples also showed the similar phase morphology, especially in domain surface roughness seemed to

be increased, and this could be an evidence for maximum elongation at break. Therefore, the critical amount for the optimized property in ternary blend system was determined as 4 phr of ESO in this study.

**Fig. 8** Fourier transform infrared spectra of Pure ESO, PLA/PBAT/PPC blends with/without ESO**Fig. 9** DSC thermograms of PLA/PBAT/PPC Blends with/without ESO**Fig. 10** TGA thermograms of PLA/PBAT/PPC Blends with/without ESO

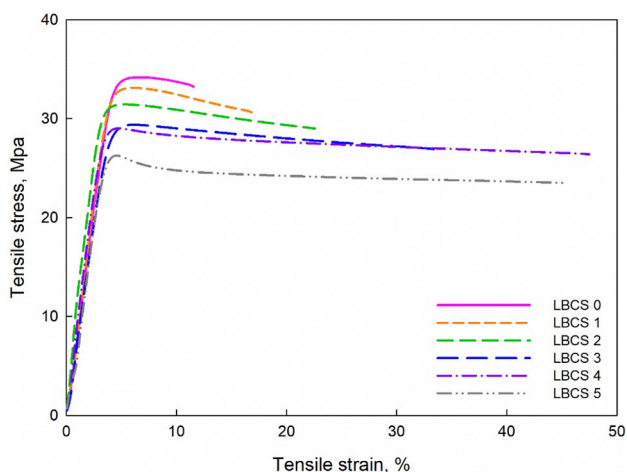


Fig. 11 Stress strain curve of PLA/PBAT/PPC Blends with/without ESO

Rheological Properties

Figure 13 presents the dynamic storage modulus and complex viscosity of PLA/PBAT/PPC ternary blend with/without ESO at 190 °C. The typical Newtonian behavior at the measured frequency range was found for all samples. There was no significant change in the slope at a low frequency, a terminal region, for all samples indicating that

the blend samples showed liquid-like behavior. The addition effect of PPC having more chain mobility to form the chain entanglement improving the elasticity of the blends was observed in Fig. 6, but ESO could not have much effect on enhancing the elasticity of ternary blends. The slope of the blends did not show much difference from that of PLA/PBAT/PPC without ESO, but the addition of ESO increased the storage modulus values of the blend due to the improved interfacial adhesion. The complex viscosity was found to increase with addition of ESO, and it could be due to chain entanglement among polymers and compatibilizer. Wang et al. reported the similar results that 0.5 wt% of TBT added to the PLA/PPC blend improved the viscosity in the lower shear rate region compared to other samples [36].

Barrier Properties

The barrier property of PLA/PBAT/PPC ternary blends with/without ESO is given in Fig. 14. As the effectiveness of PPC addition on the PLA/PBAT blends was confirmed from the Fig. 7. It was expected that the addition of ESO on the PLA/PBAT/PPC blends could improve the oxygen barrier property induced from the increased the interfacial interaction. However, it was found that the oxygen permeability increased with addition of ESO, and further increase was observed as ESO contents increased. The

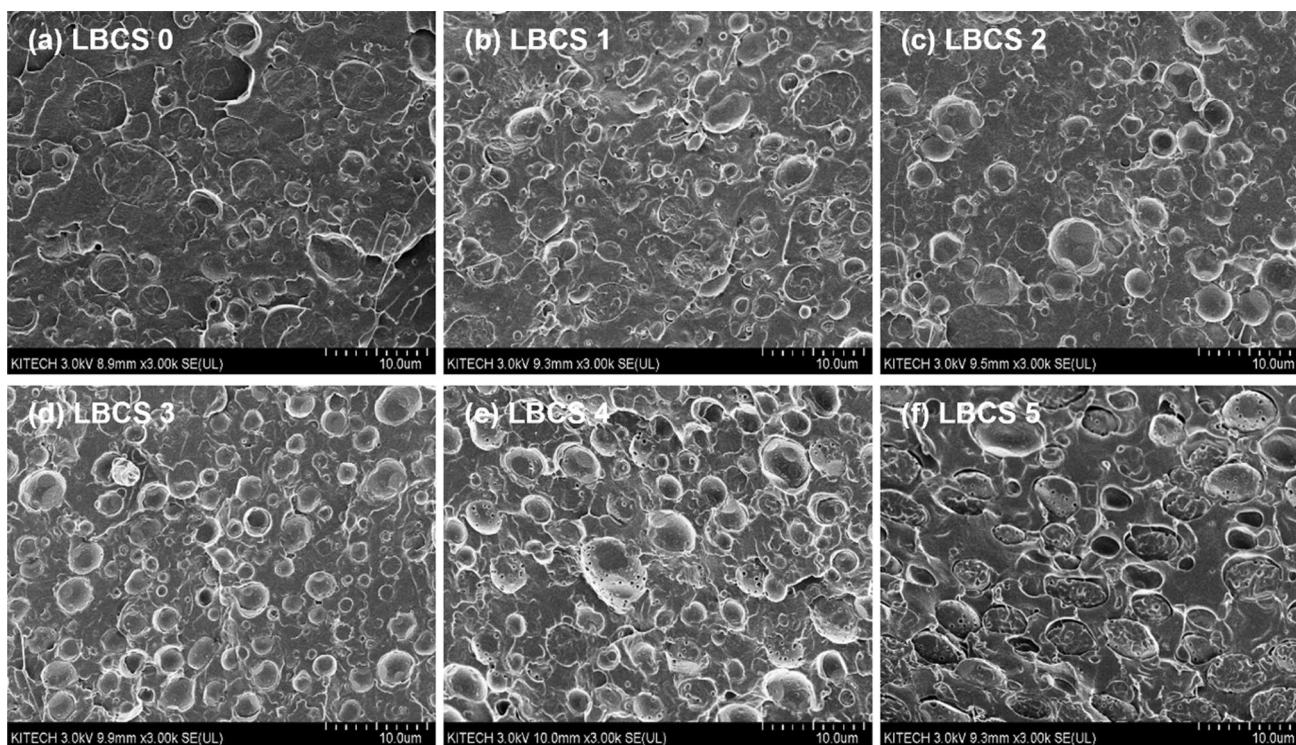


Fig. 12 SEM images cryo-fractured surfaces of PLA/PBAT/PPC Blends with/without ESO

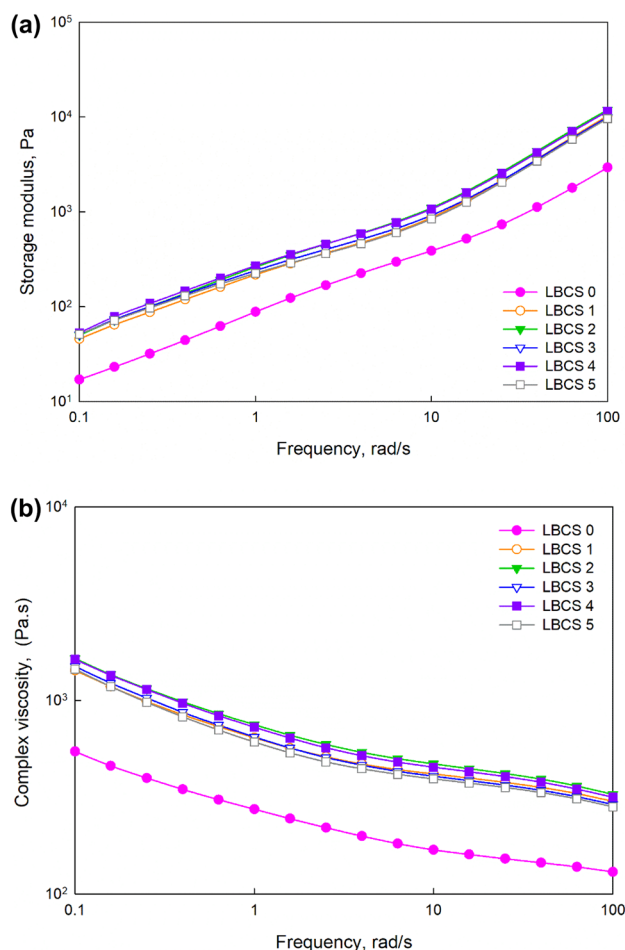


Fig. 13 Rheological properties of PLA/PBAT/PPC Blends with/without ESO **a** storage modulus G' **b** complex viscosity η^*

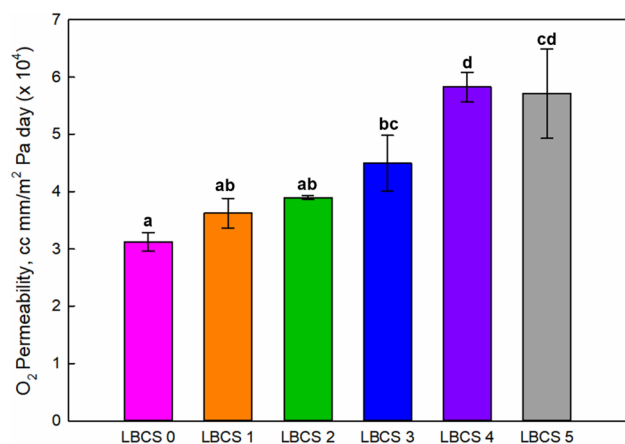
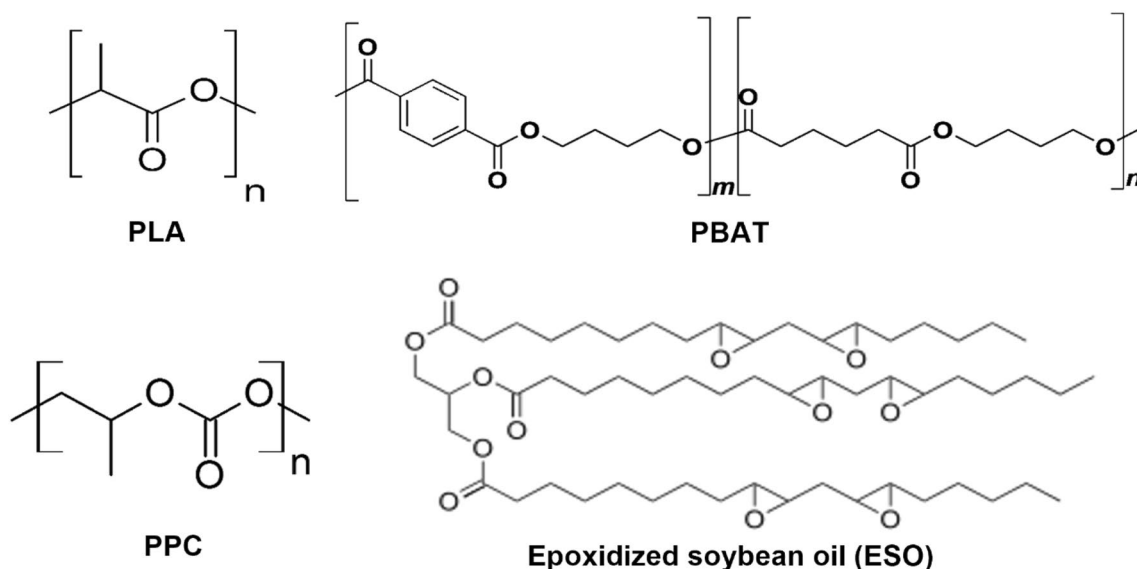


Fig. 14 Barrier properties for PLA/PBAT/PPC Blends with/without ESO

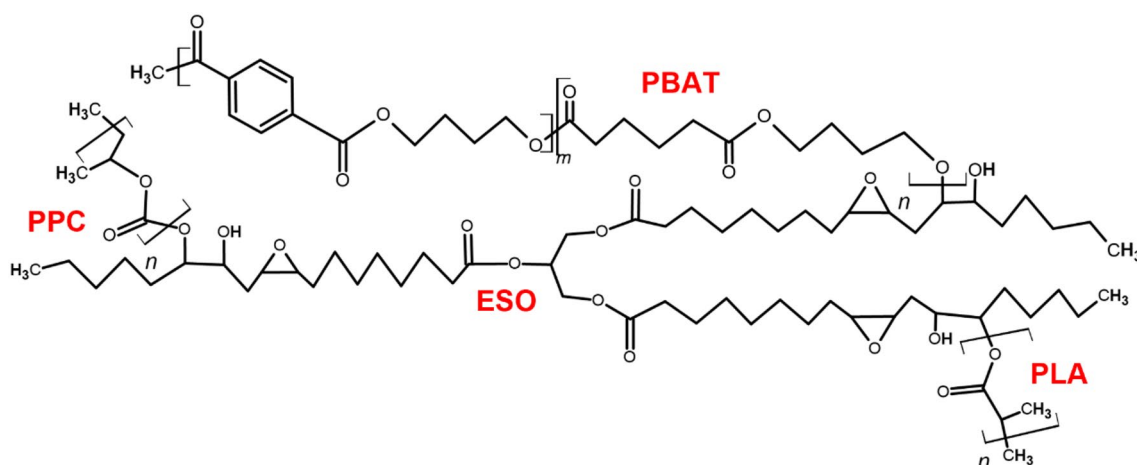
typical permeation pathway is the free volume generated among the molecular chains in polymers, and various factors has an effect on movement of gaseous permeant molecules such as the microstructure and morphology, chain entanglement, chemical structure of polymer, and processing conditions. From the mechanical properties and the morphological observation, it could be concluded that the ability to transfer the tensile stress through the interfaces in PLA/PBAT/PPC blends was enough to increase the elongation behavior, while the micro voids and cavities in the microstructure still allow the oxygen molecules penetrate through the interfaces resulting in lower barrier property. In addition, the plasticizing effect of liquid ESO in the ternary blends increasing the free volume in the blend could promote the oxygen permeation as well in this case.

Conclusions

In this study, the physical and mechanical properties of PLA, PBAT and PPC ternary blend based on an optimized ratio of PLA/PBAT was 70:30 wt% from previous studies were investigated. It was found that as the PPC contents increased, the elongation at break and thermal stability showed a decrease tendency, however the barrier properties of PLA/PBAT with the addition of PPC increased. The T_g of most compositions was dropped as compared to that of neat PLA and this could be seen that amorphous PPC could increase the chain mobility in the blends. From the mechanical, thermal and barrier properties, the LBC 10 (PPC contents 10wt%) ratio are determined for suitable compositions for the reactive compatibilization study. It was confirmed that the epoxy group of ESO reacted with carboxyl/hydroxyl groups of PLA, PBAT, PPC during melt blending process, and it was found that as the ESO contents increased, the elongation at break also considerably increased while slight reduction in the tensile strength. In case of the LBCS 4 (ESO 4 phr), elongation at break increased by about 389% as compared to the LBCS 0 without the ESO, and the 4 phr of ESO was determined for critical amount in this study. The addition of ESO did not have a significant effect on the thermal stability of the blends, and the crystallinity was also found to be increased due to the polymer chain rearrangement. Although the addition of ESO affected on increasing the elongation at break, the ESO showed a negative effect on the oxygen barrier property. This could be attributed to the combination effect with the presence of the micro voids and cavities in the microstructure in the blends and the plasticizing



Scheme 1 Chemical structures of PLA, PBAT, PPC and Epoxidized soybean oil



Scheme 2 Ring-open reaction of ESO with PLA, PBAT and PPC

effect of ESO increasing the free volume in the blends. Therefore, it could be still challenged to enhance the interaction among each polymer and compatibilizer and control the morphology and interface to acquire the better property in following further study.

Author Contributions SWH and JEC designed the concept, and JEC mainly performed overall experiments. THP and SMJ involved the sample analysis and data acquisition, and they also provide valuable comments to perform this research. JEC and SWH wrote the main manuscript and all authors reviewed the manuscript.

Funding This research was a part of the project titled Development to solve current issues in seafood distribution (Grant Number: 1525011894) funded by the Ministry of Oceans and Fisheries, Korea.

Data Availability The datasets generated during and/or analyzed during the current study are available from the corresponding author on reasonable request.

Declarations

Conflict of interest I declare that the authors have no competing interests as defined by Springer, or other interests that might be perceived to influence the results and/or discussion reported in this paper.

References

- Silva ALP, Prata JC, Walker TR, Duarte AC, Ouyang W, Barcelò D (2021) Rocha-Santos, increased plastic pollution due to COVID-19 pandemic: challenges and recommendations. *Chem Eng J* 405:126683
- Nofar M, Sacligil D, Carreau PJ, Kamal MR, Heuzey M-C (2019) Poly (lactic acid) blends: processing, properties and applications. *Int J Biol Macromol* 125:307–360
- Rasal RM, Janorkar AV, Hirt DE (2010) Poly (lactic acid) modifications. *Prog Polym Sci* 35:338–356
- Haneef I, Buys Y, Shaffar N, Shaharuddin S, Khairussihma MN (2019) Miscibility, mechanical, and thermal properties of polylactic acid/polypropylene carbonate (PLA/PPC) blends prepared by melt-mixing method. *Mater Today: Proceedings* 17:534–542
- Mahmud S, Long Y, Abu Taher M, Xiong Z, Zhang R, Zhu J (2019) Toughening polylactide by direct blending of cellulose nanocrystals and epoxidized soybean oil. *J Appl Polym Sci* 136:48221
- Zhou Y, Wang J, Cai S-Y, Wang Z-G, Zhang N-W, Ren J (2018) Effect of POE-g-GMA on mechanical, rheological and thermal properties of poly (lactic acid)/poly (propylene carbonate) blends. *Polym Bull* 75:5437–5454
- Song L, Li Y, Meng X, Wang T, Shi Y, Wang Y, Shi S, Liu L-Z (2021) Crystallization, structure and significantly improved mechanical properties of PLA/PPC blends compatibilized with PLA-PPC copolymers produced by reactions initiated with TBT or TDI. *Polymers* 13:3245–3246
- Tian X, Hu Y, Zhang J, Guo X, Bai R, Zhao L (2019) Blends of poly (l-lactide), poly (propylidene carbonate) and graphene oxide compatibilized with poly (ethylene glycol), and their mechanical properties. *J Mater Sci* 54:14975–14985
- Xia M, Shi K, Zhou M, Shen Y, Wang T (2019) Effects of chain extender and uniaxial stretching on the properties of PLA/PPC/mica composites. *Polym Adv Technol* 30:2436–2446
- Hwang SW, Park DH, Kang DH, Lee SB, Shim JK (2016) Reactive compatibilization of poly (l-lactic acid)/poly (propylene carbonate) blends: thermal, thermomechanical, and morphological properties. *J Appl Polym Sci* 133:43388
- Kim DY, Lee JB, Lee DY, Seo KH (2020) Plasticization Effect of Poly (Lactic Acid) in the Poly (Butylene Adipate-co-Terephthalate) Blown Film for Tear Resistance Improvement. *Polymers* 12:1904
- Arruda LC, Magaton M, Bretas RES, Ueki MM (2015) Influence of chain extender on mechanical, thermal and morphological properties of blown films of PLA/PBAT blends. *Polym Test* 43:27–37
- Somsunan R, Noppakoon S, Punyodom W (2019) Effect of G40 plasticizer on the properties of ternary blends of biodegradable PLA/PBS/G40. *J Polym Res* 26:1–11
- Kumar V, Sehgal R, Gupta R (2021) Blends and composites of polyhydroxyalkanoates (PHAs) and their applications. *Eur Polym J* 161:110824
- Archer E, Torretti M, Madbouly S (2021) Biodegradable polycaprolactone (PCL) based polymer and composites. *Phys Sci Rev*. <https://doi.org/10.1515/psr-2020-0074>
- Barletta M, Aversa C, Ayyoob M, Gisario A, Hamad K, Mehropouya M, Vahabi H (2022) Poly (butylene succinate)(PBS): Materials, processing, and industrial applications. *Prog Polym Sci* 8:101579
- Han X, Jin Y, Wang B, Tian H, Weng Y (2022) Reinforcing and toughening modification of PPC/PBS blends compatibilized with epoxy terminated hyperbranched polymers. *J Polym Environ* 30:461–471
- Jian J, Xiangbin Z, Xianbo H (2020) An overview on synthesis, properties and applications of poly (butylene-adipate-co-terephthalate)-PBAT. *Adv Industrial Eng Polym Res* 3:19–26
- Jiang G, Wang F, Zhang S, Huang H (2020) Structure and improved properties of PPC/PBAT blends via controlling phase morphology based on melt viscosity. *J Appl Polym Sci* 137:48924
- Luinstra GA, Borchardt E (2012) Material properties of poly (propylene carbonates). *Adv Polym Sci* 245:29–48
- Zhao L, Jia S-L, Wang Z-P, Chen Y-J, Bian J-J, Han L-J, Zhang H-L, Dong L-S (2021) Thermal, rheological and mechanical properties of biodegradable poly (propylene carbonate)/epoxidized soybean oil blends. *Chin J Polym Sci* 39:1572–1580
- Cui S, Wei P, Li L (2019) Thermal decomposition behavior of poly (propylene carbonate) in poly (propylene carbonate)/poly (vinyl alcohol) blend. *J Therm Anal Calorim* 135:2437–2446
- Zhao Y, Li Y, Xie D, Chen J (2021) Effect of chain extender on the compatibility, mechanical and gas barrier properties of poly (butylene adipate-co-terephthalate)/poly (propylene carbonate) bio-composites. *J Appl Polym Sci* 138:50487
- Lyu Y, Chen Y, Lin Z, Zhang J, Shi X (2020) Manipulating phase structure of biodegradable PLA/PBAT system: effects on dynamic rheological responses and 3D printing. *Compos Sci Technol* 200:108399
- Qiu S, Zhou Y, Waterhouse GI, Gong R, Xie J, Zhang K, Xu J (2021) Optimizing interfacial adhesion in PBAT/PLA nanocomposite for biodegradable packaging films. *Food Chem* 334:127487
- Wang B, Jin Y, Kang Ke, Yang N, Weng Y, Huang Z, Men S (2020) Investigation on compatibility of PLA/PBAT blends modified by epoxy-terminated branched polymers through chemical micro-crosslinking. *e-Polymers* 20:39–54
- Cui S, Li L, Wang Q (2016) Enhancing glass transition temperature and mechanical properties of poly (propylene carbonate) by intermacromolecular complexation with poly (vinyl alcohol). *Compos Sci Technol* 127:177–184
- Muthuraj R, Misra M, Mohanty AK (2018) Biodegradable compatibilized polymer blends for packaging applications: a literature review. *J Appl Polym Sci* 135:45726
- Pan H, Li Z, Yang J, Li X, Ai X, Hao Y, Zhang H, Dong L (2018) The effect of MDI on the structure and mechanical properties of poly (lactic acid) and poly (butylene adipate-co-butylene terephthalate) blends. *RSC Adv* 8:4610–4623
- Han Y, Shi J, Mao L, Wang Z, Zhang L (2020) Improvement of compatibility and mechanical performances of PLA/PBAT composites with epoxidized soybean oil as compatibilizer. *Ind Eng Chem Res* 59:21779–21790
- Aliotta L, Gigante V, Acucella O, Signori F, Lazzeri A (2020) Thermal, mechanical and micromechanical analysis of PLA/PBAT/POE-g-GMA extruded Ternary Blends. *Front Mater* 7:130
- Chinsirikul W, Rojsatean J, Hararak B, Kerddonfag N, Aontee A, Jaieau K, Kumsang P, Sripethdee C (2015) Flexible and tough poly(lactic acid) Films for Packaging Applications: property and processability improvement by effective reactive blending. *Packaging Technol Sci* 28:741–759
- Lins LC, Livi S, Duchet-Rumeau J, Gérard J-F (2015) Phosphonium ionic liquids as new compatibilizing agents of biopolymer blends composed of poly (butylene-adipate-co-terephthalate)/poly (lactic acid)(PBAT/PLA). *RSC advances* 5(73):559082–59092
- Jiang G, Li H, Wang F (2021) Structure of PBAT/PPC blends prepared by in-situ reactive compatibilization and properties of their blowing films. *Mater Today Commun* 27:102215
- Carbonell-Verdu A, Ferri J, Dominici F, Boronat T, Sanchez-Nacher L, Balart R, Torre L (2018) Manufacturing and compatibilization of PLA/PBAT binary blends by cottonseed oil-based derivatives. *Express Polym Lett* 12:808–823
- Wang Z, Zhang M, Liu Z, Zhang S, Cao Z, Yang W, Yang M (2018) Compatibilization of the poly (lactic acid)/poly (propylene

carbonate) blends through in situ formation of poly (lactic acid)-b-poly (propylene carbonate) copolymer. *J Appl Polym Sci* 135:46009

Publisher's Note Springer Nature remains neutral with regard to jurisdictional claims in published maps and institutional affiliations.

Springer Nature or its licensor (e.g. a society or other partner) holds exclusive rights to this article under a publishing agreement with the author(s) or other rightsholder(s); author self-archiving of the accepted manuscript version of this article is solely governed by the terms of such publishing agreement and applicable law.